JOURNAL OF AIRCRAFT
Vol. 42, No. 1, January–February 2005

# Bonded Composite Patch Design for Aircraft Structures Exhibiting Cracking and Corrosion

Madhukar Singh* and William P. Schonberg†
*University of Missouri–Rolla, Rolla, Missouri 65409*

**Many military and civilian aircraft are expected to operate beyond their designed life expectancy. As a result, the development of reliable and cost-effective repair techniques for deteriorating components in aging aircraft is of great interest. The application of bonded composite material patches to restore cracked and corroded metallic airframes has been shown to be an effective repair technique for increasing the durability and damage tolerance of the repaired structure. Composite Repair of Aircraft Structures (CRAS) is a computer program that is currently being used to design bonded patches for damaged metallic structures. The results are presented for a study whose objective was to extend the applicability of the CRAS program to include bonded patch design for aircraft structures that have sustained adjacent cracking and corrosion damage. Patch designs were developed for three different cracking and corrosion configurations. Composite patches were manufactured according to the designs developed and applied to damaged aluminum panels using a hot-bonding device. Patched and unpatched panels were loaded to failure using a material testing system (MTS) 880 machine. In all cases the failure loads of the patched panels exceeded those of corresponding unpatched panels. These results validated the patch design procedure developed herein for the configurations considered.**

## Introduction

MANY military and civilian aircraft are expected to operate beyond their designed life expectancy because of economic constraints and the competitive global economy. For example, the U.S. Air Force C-141 fleet is expected to last beyond its planned retirement in 2003 (i.e., at least a 38-year life span[1]). As a result, the development of a reliable and cost-effective repair technique for damaged aircraft components is of great national and international interest.[2,3] Deteriorating aircraft components could easily lead to catastrophic failures and loss of human life if not adequately repaired.

Traditional repair techniques include the mechanical fastening or riveting of metallic patches or doublers. These techniques have been used for repairing cracked structures, multisite or widespread damage, corrosion, and many other common flaws detected during inspection of aging aircraft. Over the past few years, bonded composite patches have begun to be used with increasing frequency to repair such damage.

Bonded repairs offer several advantages over mechanically fastened repairs. Mechanically fastened repairs introduce stress concentrations from the fastener holes; adhesive bonding provides more uniform and efficient load transfer into the repair patch than do mechanical fasteners; an adhesive joint is often lighter than a mechanical fastener, an important consideration in the aircraft industry; the adhesive acts as a joint sealant, preventing water and air from penetrating between the adherents; and an adhesive joint can be made aerodynamically smooth, whereas a mechanical fastener may act as a protrusion into airflow.

The application of bonded composite materials patches to restore cracked or corroded metallic airframes in military aircraft has been shown to be a durable and cost-effective repair technique for increasing the life span and damage tolerance of the repaired structure.[4,5] These repairs have been shown to alter the load path, bridge the crack, and reduce stress intensity factors, thus retarding crack growth.[6–10] Adhesively bonded repairs can be applied to the aircraft structure quickly and onsite, thereby drastically reducing the large costs normally associated with aircraft disassembly and downtime.[4,11] Successful demonstrations of bonded patch repair have been performed on the F-16 fighter and the C-5A transport aircraft[5] as well as the Mirage III fighter.[11,12]

The Composite Repair of Aircraft Structures (CRAS) computer software is an analysis/design code that is currently used to design bonded patches for damaged metallic structures.[2] Damage may be either through-the-skin cracks or elliptical grind-outs of corroded areas. The patch designs provided by the CRAS are based on user input of the material properties for the skin, patch, adhesive, ultimate static loads, damage configuration (e.g., crack length, grind-out diameter and depth), and the patch shape. Through an iterative process, CRAS develops a design that satisfies all static strength and crack growth requirements with a reasonable patch size and thickness.

The CRAS software package is fairly versatile; however, the variety of damage configurations and applied load combinations to which it can be applied is somewhat limited. For example, in its current configuration, the CRAS program is able to design patches either for corroded structures or for cracked structures, but not for structures exhibiting simultaneous and adjacent cracking and corrosion damage. In practical applications the chances of getting either only corrosion or only cracking are fairly low. Wherever there is predominant crack damage in an aircraft structure, the possibility of corrosion damage is fairly high. Similarly, wherever there is predominant corrosion damage, the possibility of corrosion-induced crack damage is also fairly high. However, at present, the CRAS program cannot design patches for structures having adjacent cracking and corrosion.

This paper presents the results of a study whose objective was to extend the applicability of the CRAS program to include bonded patch design for aircraft structures having adjacent cracking and corrosion damage. Because an early, developmental version of the CRAS program was used, the full capabilities of later versions of the program were not available or used. The validity of the developed design process was tested by comparing the failure loads for corresponding patched and unpatched panels.

## Theoretical Development

Although there can be many orientations for the crack and corrosion to occur simultaneously, for simplicity the crack and corrosion

Received 8 April 2003; revision received 22 October 2003; accepted for publication 1 November 2003. 

*Graduate Student, Mechanical Engineering Department.
†Professor, Civil Engineering Department, 1870 Miner Circle; wschon@umr.edu. Associate Fellow AIAA.

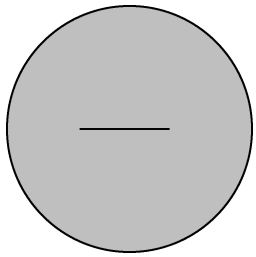

**a) Case 1: Corrosion grind-out with one internal crack**

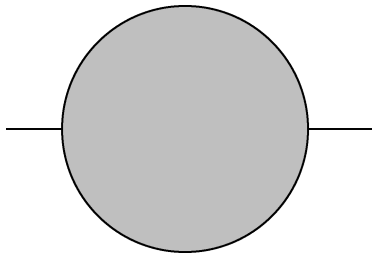

**b) Case 2: Corrosion grind-out with two external cracks**

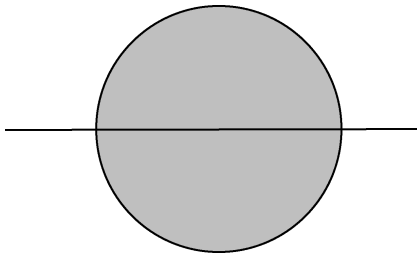

**c) Case 3: Corrosion grind-out with one through crack**

**Fig. 1 Combined crack + corrosion damage configurations considered.**

are considered to be located centrally and symmetrically with respect to the applied load. Three different crack/corrosion damage configurations were considered in this study: 1) case 1 corrosion grind-out with one internal crack (see Fig. 1a); 2) case 2, corrosion grind-out with two external cracks (see Fig. 1b); and 3) case 3, corrosion grind-out with one through-crack (see Fig. 1c).

A computer code was written in C++ to obtain patch designs for the three crack/corrosion damage configurations considered based on the CRAS design criteria as described in Ref. 13. Patch design consisted of two fundamental components, patch dimensions and number of plies, and was based on user input of material properties for the skin, patch and adhesive, the applied load, damage configuration (crack length, corrosion grind-out diameter and depth), and the kind of damage configuration (i.e., whether the damage is corrosion grind-out with one internal crack, corrosion grind-out with two external cracks, or corrosion grind-out with one through crack). Patch designs were obtained using the following sequence of calculations.

*Step 1: Calculate the Number of Plies*

In this step we calculate preliminary patch design parameters and use them to determine the number of plies in the final patch design. First, patch dimensions and the number of plies Nply were obtained considering only the crack and ignoring the presence of the corrosion. Next, the situation was reversed: patch dimensions and the number of plies Nply1 were obtained for corrosion only, ignoring the presence of the crack(s). Then, when we compared Nply and Nply1, one of the three following possibilities ensued.

*Nply > Nply1.* In this case we let Nply1 = Nply; that is, the value of Nply1 was replaced by Nply. The design process for corrosion only was run again using Nply as the number of plies to obtain a new set of corrosion patch dimensions. We now have two sets of patch dimensions: one for the crack-only case and the other for the corrosion-only case, but both with the same number of plies Nply, which is the number of plies in the final patch design. We then moved to the next step in the design process, in which we calculated the final dimensions of the patch for the actual combined crack/corrosion case being considered.

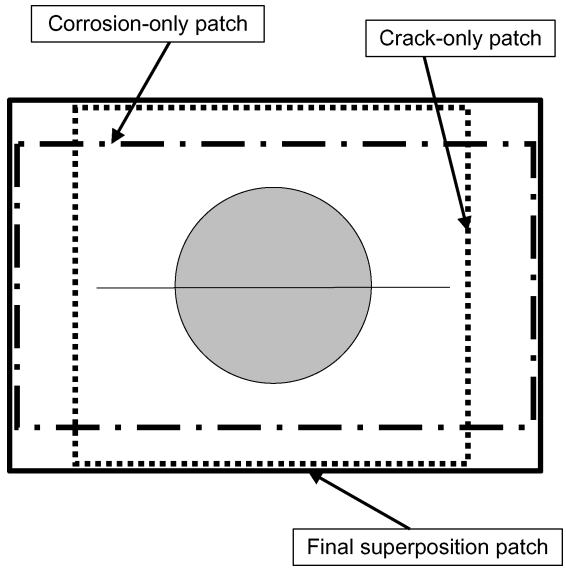


**Fig. 2 Superposition approach for final patch dimensions.**

*Nply1 > Nply.* In this case we let Nply = Nply1; that is, the value of Nply was replaced by Nply1. The design process for cracking only was run again using Nply1 as the number of plies to obtain a new set of crack patch dimensions. This likewise resulted in two sets of patch dimensions, one for the crack-only case and one for the corrosion-only case, but again both with the same number of plies Nply1, which is the number of plies in the final patch design. We then moved to the next step in the design process, in which we calculated the final dimensions of the patch for the actual combined crack/corrosion case being considered.

*Nply1 = Nply.* In this case we move directly to the next step of the design process in which the final dimensions of the patch were obtained for the actual combined crack/corrosion case under consideration.

*Step 2: Calculate Final Patch Dimensions*

In this step we used the two sets of preliminary crack-only and corrosion-only patch designs obtained previously to determine the final patch dimensions for the actual crack/corrosion case being considered. These final patch dimensions were obtained by comparing the patch lengths and widths in the individual designs. In cases 1 and 2, the final patch length and width are greater than the individual lengths and widths. In case 3, the final length of the patch is the greater of the two lengths; however, the final width of the patch in case 3, from geometric considerations, is given by the equation

$$W_f = W1 + L_{\mathrm{cr}} + W + d \tag{1}$$

where $L_{\mathrm{cr}}$ is the length of each crack, $W1$ and $W$ are the corrosion-only and crack-only patch widths, and $d$ is the diameter of the corrosion grind-out. Figure 2 illustrates this superposition approach to obtaining the final patch design dimensions.

## Experimental Testing and Validation

The patch design process described earlier was validated by performing a series of static ramp-to-failure tests on patched and unpatched panels for six different damage configurations using a material testing system (MTS) 880 machine; fatigue testing was not considered in this study and is reserved for a follow-on activity.

**Table 1 Test matrix**

| Configuration | Specimen ID no. | Crack length, mm | Grind-out diameter, mm | Grind-out depth mm |
|---|---|---|---|---|
| Corrosion grind-out with one internal crack | SCC1-1 | 6.35 | 25.4 | 0.81 |
| | SCC1-2 | 12.7 | | |
| Corrosion grind-out with two external cracks | SCC2-1 | 6.35 ea | 25.4 | 0.81 |
| | SCC2-2 | 12.7 ea | | |
| Corrosion grind-out with one through crack | SCC3-1 | 38.1 | 25.4 | 0.81 |
| | SCC3-2 | 50.8 | | |

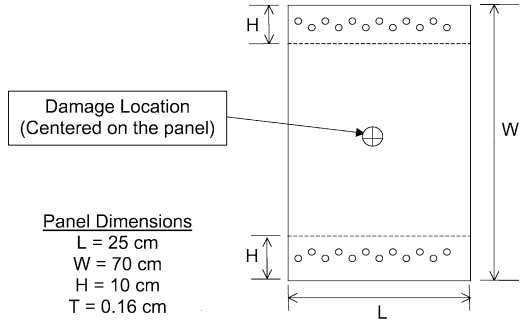


**Fig. 3 Generic test specimen.**

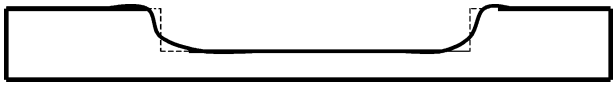

**Fig. 4 Grind-out cross section.**

Table 1 shows the test matrix for the different damage configurations considered.

### Preparation of the Test Panels

All of the test panels were made of aluminum 2024-T3, were 1.6 mm thick, and were all machined out of the same lot. Twelve holes were drilled into the panels at each end to allow the panels to be held by the fixture using nuts and bolts. Two identical damaged specimens were prepared for each test. One specimen was tested without a patch and one was tested after a patch had been applied to the panel. The crack damage was formed using an electrical discharge machining (EDM) machine whereas the corrosion grind-out was obtained using a milling machine. Figure 3 shows a generic aluminum panel with dimensions and the location of damage and the boltholes. The walls of the grind-out are sloped and rounded approximately as shown in Fig. 4 to prevent any stress concentration at the edge of the grind-out.

After the precracking and grinding was completed, the grind-out areas were filled with Devcon WR-2 wear-resistant putty. The putty was prepared by mixing hardener and resin in the ratio of 1:4 by volume. Before applying the putty, the grind-out area was cleaned with acetone. After the putty hardened, its surface was smoothened with a fine sandpaper in preparation for patch application. Figure 5 shows the damage area before and after application of the putty had been applied to the grind-out area of the panel.

### Patch Design Parameters and Preparation

Patches were designed for each of the cases shown in Table 1 using a design load of 94.7 kN = 23.3 kPa for the panel thickness used. Table 2 presents the design parameters for each of the patches for the different damage configurations that were obtained using the procedure described in the previous section. Design parameters A–D are shown in Fig. 6. We note that the dimensions in Table 2 are for the largest, or base, ply in each patch. The dimensions of the subsequent plies are adjusted based an assumed 20:1 taper ratio. The ply material in each case was unidirectional Boron Epoxy 5521 tape; the thickness of the tape was 0.127 mm.

**Table 2 Final patch design parameters**

| Specimen ID | No. of plies | Dimensions, mm A | B | C | D |
|---|---|---|---|---|---|
| SCC1-1 | 5 | 71.6 | 114.8 | 24.6 | 50.8 |
| SCC1-2 | 5 | 71.6 | 114.8 | 24.6 | 50.8 |
| SCC2-1 | 5 | 71.9 | 114.8 | 24.6 | 50.8 |
| SCC2-2 | 5 | 78.2 | 114.8 | 24.6 | 50.8 |
| SCC3-1 | 5 | 71.6 | 114.8 | 26.9 | 50.8 |
| SCC3-2 | 5 | 71.6 | 114.8 | 24.6 | 50.8 |

**a) Damaged panel without putty**

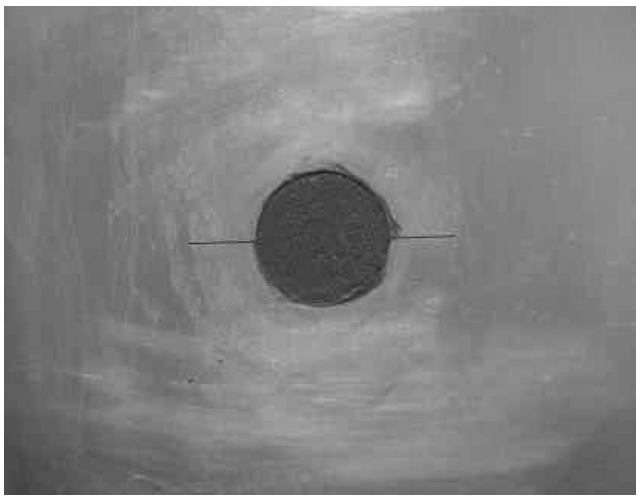

**b) Damaged panel with putty**

**Fig. 5 Application of putty to damaged panel.**

A template for each patch design was drawn using Auto-Cad and then transferred to polythene sheets. These sheets were used because they did not stick to the prepeg tape when the tape was cut manually to the design specifications. We noted that the boron/epoxy tape became soft and sticky and the boron fibers tended to peel apart at room temperature, which made it difficult to cut. To overcome this difficulty, the boron/epoxy tape was kept in a freezer until it was ready to be cut. As each ply of a boron/epoxy patch was cut, it was put back into the freezer immediately so that it remained hard and the boron fibers remained intact. After cutting all the plies of the patch, the plies were aligned carefully one above the other and cured.

### Patch Curing

A device called a hot-bonder was used for precuring the boron/epoxy patches. The precured patches were then bonded to the structure in a separate operation, usually at somewhat lower temperature. This two-step process was preferred because it minimizes

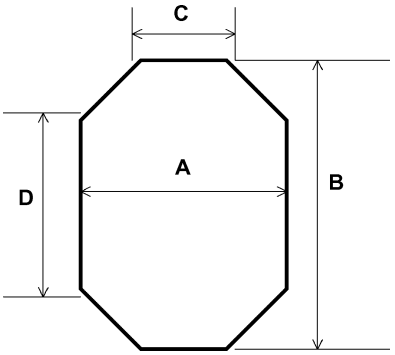


**Fig. 6 Patch design parameters A–D.**

residual thermal stresses in the repaired structure. The following paragraphs describe the operation of the hot-bonder device and the patch-curing process.

To begin, a peel ply was placed over an aluminum plate, which acted as a worktable base. The patch was placed over the peel ply and a second layer of peel ply was placed over the patch. Then a layer of breather material was placed over the second peel ply. The purpose of the breather material was to help control the suction of air during the vacuum process. The vacuum nozzle was placed over the breather material. Tacky tape was fixed around this entire setup on the worktable. Two thermocouples were placed symmetrically along the two adjacent sides of the patch. A vacuum bag was placed over the breather material and was pressed firmly over the tacky tape to ensure that there would be no air leakage during the vacuum process. A heat blanket was placed over the vacuum bag, taking care to ensure that the heat blanket was not placed directly over the tacky tape.

**Patch Application to the Panel**

FM-73 adhesive, which has a cure temperature between 200 and 250°F, was used to bond each patch to the aluminum test panels. Adhesives that cure between 200 and 250°F have good strength and stiffness and adequate moisture resistance and are therefore most desirable for composite patching.[13] Good adhesion of a bonded patch to the structural surface is critical to the long-term durability of a repair as well as assuring good load transfer through the bondline.

Prior to patch installation, the damaged panels were cleaned to remove the oil, paints, and other sticky material. Then the damaged regions were cleaned thoroughly with acetone. Preparing the specimen in this manner removes the aluminum oxide layer, which is necessary for the formation of a good adhesive bond. A piece of FM-73 adhesive was cut to approximately the same size of the largest (i.e., bottom-most) ply of a patch. In each case the thickness of the adhesive layer was 0.10 mm. The patch and the adhesive were placed over the damaged area to be repaired. The hot-bonder was again used for curing the adhesive using the procedure described earlier. Although a double ramp cycle was used for precuring the boron/epoxy patches, only a single ramp cycle was used for bonding the patch to the aluminum substrate. The difference in cycle type is due to the following considerations.

While curing, both the patch pressure and temperature are critical factors. Boron/epoxy patches are normally cured in an autoclave where the pressure applied is 170 kPa; however, here the patch was cured using a hot-bonder, which can apply a maximum pressure of 60 kPa. Therefore, to obtain the same properties of the patch as would have been obtained in an autoclave, a double ramp cycle was used. However, during bonding only patch temperature is the critical factor; the pressure of 9 psi applied by the hot-bonder is already at the level necessary to obtain a perfect bond between the patch and the substrate material. Hence, patch bonding required only a single ramp cycle whereas patch curing required a double ramp cycle.

**Strain Gauge Placement**

EA-06-250BG-120 strain gauges were used to record the strain developed near the damaged region. The EA series of strain gauges

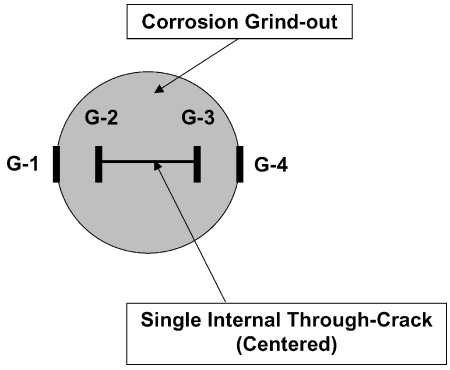


**a) Strain gauge locations for specimen type SCC1**

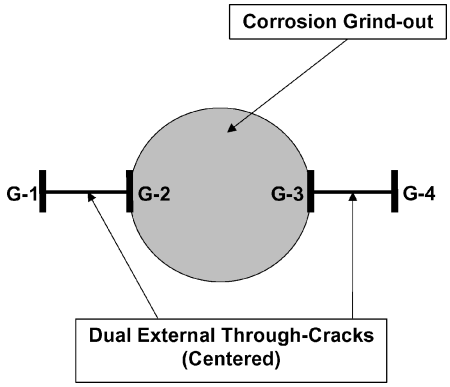


**b) Strain gauge locations for specimen type SCC2**

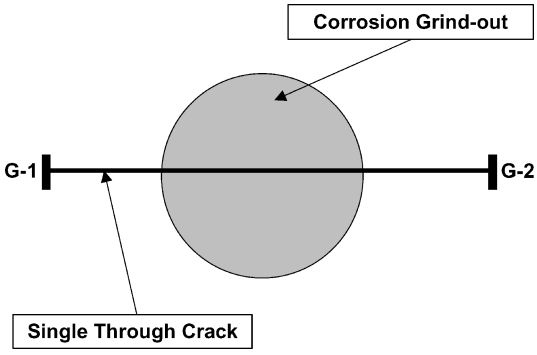


**c) Strain gauge locations for specimen type SCC3**

**Fig. 7 Strain gauge locations.**

is a general-purpose family of constant strain gauges used in experimental stress and strain analysis. These strain gauges are of the open-faced construction type with a 1-mil (0.025-mm) tough, flexible polyimide backing. Their temperature range is −100 to 350°F for special or short-term exposure. This temperature range is critical while soldering the lead wires to the strain gauges. The leads were attached using tin/lead solder while M-bond 200 was used for bonding the strain gauge to the test panels. The strain gauges were applied to the unpatched sides of the patched panels at each of the crack tips where the stress concentrations were expected to be the highest (see Fig. 7). The region where each strain gauge was applied was first cleaned with a fine sandpaper. Then a coating was applied to prevent the oxidation of the pure aluminum with the air.

**Test Goals and Criteria**

The objective of each test conducted was to obtain the failure load for a particular damage configuration with and without a patch. Since the data were read using a load-vs-strain data acquisition system, failure was considered to occur in a test when either load values dropped precipitously or began to exhibit erratic behavior with increasing strain (thereby indicating either specimen failure,

loss of adhesion between the patch and the test panel, or a test fixture irregularity). Loads applied to the test specimen were ramped up monotonically in a nonshocking, nonheating manner until the specimen failed. The rate of load application was 16.2 N/s. The next section presents and discusses the results of the tests performed on the patched and unpatched specimens.

## Results and Discussion

Table 3 shows the final outcome of each of test, that is, the load at which the panel failed and the type of failure that occurred (e.g., a crack extension failure, CE, or a bolt bearing failure, BB). In Table 3 we see that in all cases the failure load for the patched specimen exceeded that of the corresponding unpatched specimen. In the case of specimen SCC3-2, the difference between the two failure loads was just over 57%. This is a significant increase in specimen strength due to the presence of the patch. Although all of the unpatched specimens had crack extension failures, only two patched specimens (SCC1-2 and SCC3-2) had crack extension failure; the rest of the patched specimens had bolt bearing failures. However, even in those cases where bolthole failure occurred, the patched specimens outperformed their unpatched counterparts. These results clearly validate the design process developed for the case of combined cracking and corrosion considered in this study.

Figures 8 and 9 show crack extension and bolt bearing failures of a patched specimen, respectively. In Fig. 8 we can see that the initial failure of a specimen that ultimately failed by crack extension occurred in the adhesive while the boron/epoxy composite patch remained intact. Once the adhesive failed (most likely in shear), the patch was no longer attached to the panel. Crack extension and complete panel failure followed shortly thereafter.

From Fig. 9 we see from the elongated boltholes that the bolt bearing failures likely occurred due to excessive bearing stresses along the edges of the boltholes as the specimens slipped and the bolts came in contact with the boltholes. These stresses were apparently higher than the stresses developed at the central damaged area and resulted in failure of the specimens along the boltholes. A possible reason for the bolt bearing failures is that the bolts were not torqued high enough to prevent slippage at the boltholes. Table 4 gives the bolt torque applied for each test.

**Table 3 Test results for corrosion + cracking tests**

| Specimen ID | Patched? (Y/N) | Test results | |
|---|---|---|---|
| | | $P_{fail}$ (kN) | Failure type |
| SCC1-1 | N | 134.8 | CE |
| | Y | 142.8 | BB |
| SCC1-2 | N | 132.6 | CE |
| | Y | 161.0 | BB |
| SCC2-1 | N | 124.9 | CE |
| | Y | 159.7 | CE |
| SCC2-2 | N | 110.3 | CE |
| | Y | 163.2 | BB |
| SCC3-1 | N | 112.5 | CE |
| | Y | 146.8 | BB |
| SCC3-2 | N | 101.8 | CE |
| | Y | 160.1 | CE |

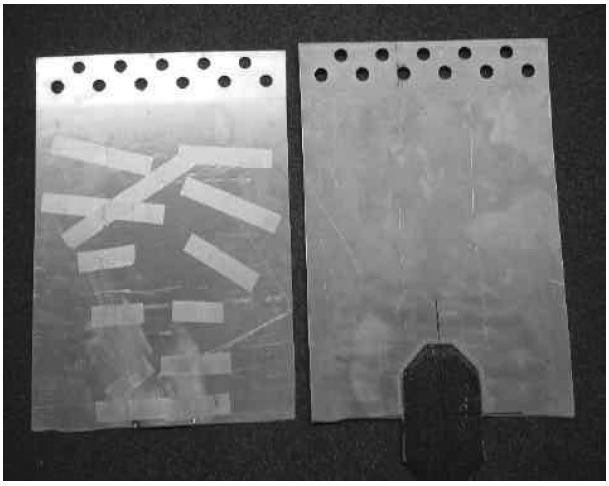

**Fig. 8 Crack extension failure.**

**Table 4 Bolt torque data**

| Specimen ID | Patched? Y/N | Torque on the bolts |
|---|---|---|
| SCC1-1 | N | 81 N·m |
| | Y | 81 N·m |
| SCC1-2 | N | 81 N·m |
| | Y | 95 N·m |
| SCC2-1 | N | 81 N·m |
| | Y | 136 N·m |
| SCC2-2 | N | 81 N·m |
| | Y | 136 ·m |
| SCC3-1 | N | 81 N·m |
| | Y | Inner-row bolts were tightened to 68 N·m; Outer-row bolts were tightened to 95 N·m |
| SCC3-2 | N | 81 N·m |
| | Y | 136 N·m |

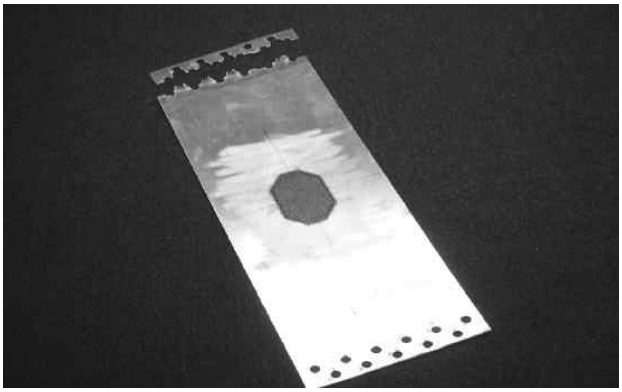

**Fig. 9 Bolt bearing failure.**

The bolt torque applied on all unpatched specimens was 81 N·m. All unpatched specimens failed at the middle; hence, the torque on the unpatched specimen was unchanged from one test to the next. The testing on the patched specimens was begun by applying a torque of 81 N·m on the patched panel SCC1-1. However, that specimen exhibited a bolt bearing failure. In an attempt to prevent this failure from happening again, the torque was increased in subsequent tests involving patched specimens. In the next test, using patched specimen SCC1-2, the bolt torque was increased to 95 N·m, but the specimen still failed at the boltholes. Bolt torque was further increased to 136 N·m for the next test with patched specimen SCC2-1. The specimen failed at the middle, and so it was thought that this torque would be high enough to prevent further bolt bearing failures. Therefore, for the next test, which involved patched specimen SCC2-2, the bolt torque was kept at 136 N·m; however, the specimen again failed at the bolts. For the next text (patched specimen SCC3-1) the inner-row bolts were tightened to 68 N·m and the outer-row bolts were tightened to 95 N·m. The specimen still failed at the bolts. Finally, for the last test (patched specimen SCC3-2), the bolt torque applied was again 136 N·m and the specimen failed at the middle. As can be seen from this discussion, the attempts to prevent bolt bearing failures were not always successful. This is an issue that future work in this area will need to address.

Figures 10 and 11 show typical load-vs-strain graphs for corresponding pairs of patched and unpatched panels, respectively. The units of load are pounds and the units of strain are microstrain. In Fig. 10 we see that the load-vs-strain curve for the unpatched specimen is smooth until the failure point. In contrast, the load-vs-strain

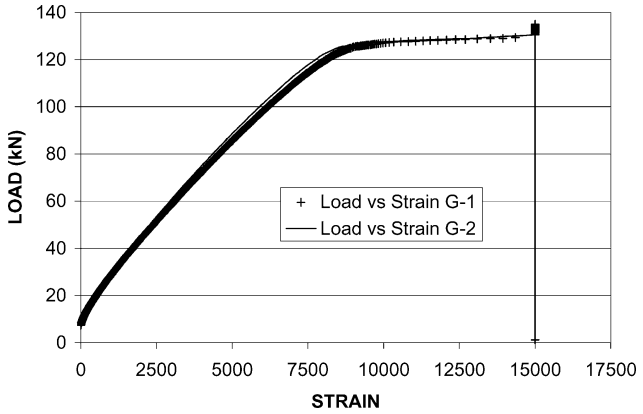


**Fig. 10 Load vs strain plot for unpatched panel SCC1-1 (strain gauge locations G-1 and G-2).**

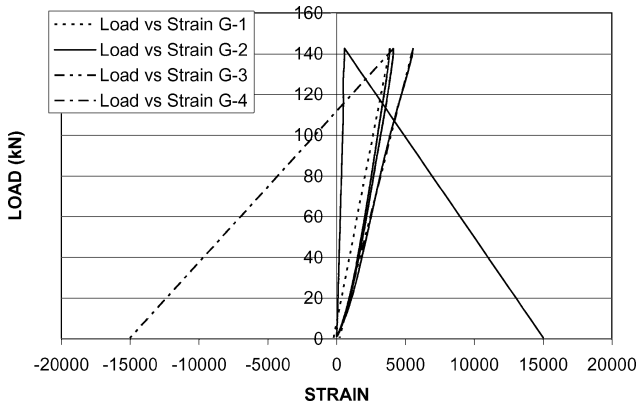


**Fig. 11 Load vs strain plot for patched panel SCC1-1 (strain gauge locations G-1, G-2, G-3, G-4).**

curve for the patch specimens in Fig. 11 is erratic. These curves are typical of those in tests of the unpatched (and patched) specimens that failed by crack extension and the patched specimens that showed bolt bearing failures, respectively. A possible explanation for this is that the unpatched specimen failed suddenly at the middle of the specimen due to crack elongation. However, the patched specimen produced an irregular curve, because there were numerous bolt slippages occurring throughout the test resulting ultimately in a bolt bearing failure.

## Conclusions

Aging military and civilian aircraft are likely to have adjacent crack and corrosion damage. A reliable and cost-effective repair technique for such damage does not yet exist. The CRAS software can be used to design patches for either corroded structures or cracked structures. However, the CRAS software cannot design patches for structures having adjacent crack and corrosion damage.

A preliminary version of the CRAS program was used to develop a patch design process for aluminum panels having adjacent crack and corrosion damage. A computer code was written to obtain the patch design for three different damage configurations: corrosion grind-out with one internal crack, corrosion grind-out with two external cracks, and corrosion grind-out with one through crack. The validity of the patch design process was assessed by performing static ramp-to-failure tests on patched and unpatched panels.

The results obtained from the tests showed that in all the cases the failure load for the patched specimen exceeded that of the corresponding unpatched specimen. In one case, the difference between the two failure loads was just over 57%. This was a significant increase in specimen strength. Some of the patched specimens failed at the boltholes. However, even in these cases the patched specimens outperformed their unpatched counterparts. These results demonstrate the validity of the design process presented herein for adjacent cracking and corrosion damage.

## Acknowledgments

The authors acknowledge the support provided by the U.S. Air Force under contract AFRL-UTC-00-S442-026-C1 (Mark Derriso, technical advisor) that made this project possible. The authors are also grateful for the many helpful comments and suggestions provided by Paul Heaton and Cong Duong of the Boeing Corporation and by Barry Spigel of the Southwest Research Institute.

## References

[1]Naboulsi, S., and Mall, S., "Methodology to Analyse Aerospace Structures Repaired with a Bonded Composite Patch," *Journal of Strain Analysis*, Vol. 34, No. 6, 1999, pp. 395–411.

[2]*CRAS Software User's Manual Version 0.3*, The Boeing Co., St. Louis, MO, Dec. 2000.

[3]Davis, M. J., Composite Materials and Adhesive Bonded Repairs, RAAF Standard Engineering C5033, Directorate of Technical Airworthiness, Royal Australian Air Force, Melbourne, Australia, 1995.

[4]Fredell, R., Guijt, C., and Mazza, J., "An Integrated Bonded Repair System: A Reliable Means of Giving New Life to Aging Airframes," *Applied Composite Materials*, Vol. 6, No. 4, 1999, pp. 269–277.

[5]Bealson, E., "Bonded Doublers for Aircraft Structural Repair," *Aerospace Engineering*, Vol. 15, No. 7, 1995, pp. 13–19.

[6]Aglan, H., Rowell, T., Ahmed, T., and Thomas, R., "Durability Assessment of Composite Repairs Bonded to Aircraft Structures," *Journal of Adhesion Science and Technology*, Vol. 13, No. 1, 1999, pp. 127–148.

[7]Caruso, R. P., "Boron/Epoxy Composites for Aircraft Structural Repair," *Composite Polymers*, Vol. 4, No. 4, 1991, pp. 242–249.

[8]Davis, M., Kearns, J., and Wilkin, M. O., "Bonded Repair to Cracking in Primary Structure: A Case Study," *Proceedings of the PICAST 2—AAC 6 Conference*, Melbourne, Australia, March 1995.

[9]Schubbe, J. J., and Mall, S., "Investigation of a Cracked Thick Aluminum Panel Repaired with a Bonded Composite Patch," *Engineering Fracture Mechanics*, Vol. 63, 1999, pp. 305–323.

[10]Naboulsi, S., and Mall, S., "Analysis of Cracked Metallic Structure with Imperfectly Bonded Composite Patch," AIAA Paper 97-1363, April 1997.

[11]Baker, A. A., Callinan, R. J., Davis, M. J., Jones, R., and Williams, J. G., "Repair of Mirage III Aircraft Using the BFRP Crack-Patching Technique," *Theoretical and Applied Fracture Mechanics*, Vol. 2, 1984, pp. 1–15.

[12]Jones, R., Davis, M., Callinan, R. J., and Mallinson, G. D., "Crack Patching: Analysis and Design," *Journal of Structural Mechanics*, Vol. 10, No. 2, 1982, pp. 177–190.

[13]"Guidelines for Composite Repair of Metallic Structure (CRMS)," Rept. No. AFRL-WP-TR-1998-4113, Wright Patterson AFB, Dayton, OH, 1998.